Chemistry of Metals and Alloys

Chem. Met. Alloys 14 (2021) 48-57
Ivan Franko National University of Lviv
www.chemetal-journal.org

Isothermal section of the Tb–Cu–Sn system at 670 K

Lyubov ROMAKA[1]*, Vitaliy ROMAKA[2], Mariya KONYK[1], Yuriy STADNYK[1]

[1] *Department of Inorganic Chemistry, Ivan Franko National University of Lviv, Kyryla i Mefodiya St. 6, 79005 Lviv, Ukraine*
[2] *Chair of Inorganic Chemistry, Technische Universität Dresden, Bergstrasse 66, 01069 Dresden, Germany*
* *Corresponding author. E-mail: lyubov.romaka@gmail.com*

Received November 30, 2021; accepted December 29, 2021; available on-line April 1, 2022
https://doi.org/10.30970/cma14.0420

The phase relations in the ternary system Tb–Cu–Sn have been studied at 670 K over the whole concentration range by X-ray powder diffraction and energy-dispersive X-ray spectroscopy. The phase equilibria at 670 K are characterized by the formation of five ternary compounds: TbCuSn (LiGaGe-type, space group *P*6$_3$*mc*, *a* = 0.4517(2), *c* = 0.7272(3) nm), Tb$_3$Cu$_4$Sn$_4$ (Gd$_3$Cu$_4$Ge$_4$-type, space group *Immm*, *a* = 0.4421(3), *b* = 0.6939(3), *c* = 1.4547(5) nm), TbCu$_5$Sn (CeCu$_5$Au-type, space group *Pnma*, *a* = 0.82205(1), *b* = 0.49789(3), *c* = 1.05766(6) nm), Tb$_{1.9}$Cu$_{9.2}$Sn$_{2.8}$ (Dy$_{1.9}$Cu$_{9.2}$Sn$_{2.8}$-type, space group *P*6$_3$/*mmc*, *a* = 0.50355(9), *c* = 2.0414(6) nm) and Tb$_2$Cu$_{3.5}$Sn$_{5.5}$ (Sm$_2$Cu$_4$Sn$_5$-type, space group *I*4*mm*, *a* = 0.4404(4), *b* = 2.5854(3) nm).

Intermetallics / Phase diagrams / X-ray diffraction / Crystal structure

1. Introduction

Studies of the phase relations in metallic systems by isothermal sections at selected temperatures reveal information on the formation, stability, homogeneity ranges, and crystal structures of the intermetallic compounds. The ternary systems with rare-earth metals, copper and tin have been studied for most rare earths [1-15] except Eu, Tb, and Tm. In the {Eu,Tb,Tm}–Cu–Sn systems only individual ternary compounds have been studied. An analysis of the studied *R*–Cu–Sn systems (*R* = rare-earth element) shows a large variety of stoichiometries and crystal structures of the intermediate ternary phases. Equiatomic *R*CuSn compounds exist with all rare earths and yttrium, but depending on the valence state and atomic size of the rare-earth element they crystallize in different structure types: LiGaGe-type (or CaIn$_2$-type) (Y, La-Sm, Gd-Er, Lu) [16-19], CeCu$_2$-type (Eu) [20], TiNiSi-type (Yb) [21], and ZrBeSi-type (La, Ce) [16,22]. Sebastian *et al.* [23] report two structural modifications of the CeCuSn stannide: a high-temperature form (β-CeCuSn) with ZrBeSi-type and a low-temperature form (α-CeCuSn) with NdPtSb-type, which is formed after annealing at 973 K. Other isotypic series, $R_3Cu_4Sn_4$ ($Gd_3Cu_4Ge_4$-type), $R_{1.9}Cu_{9.2}Sn_{2.8}$ ($Dy_{1.9}Cu_{9.2}Sn_{2.8}$-type), and RCu_5Sn ($CeCu_5Au$, $CeCu_6$ structure types) have representatives among most rare earths [24,25], while the $RCu_{1-x}Sn_2$ ($CeNiSi_2$-type), RCu_2Sn_2 ($CaBe_2Ge_2$-type) [25] and RCu_9Sn_4 ($LaFe_9Si_4$-type) compounds [26,27] are typical for the systems containing light rare-earths.

An analysis of the studied *R*–Cu–Sn ternary systems with rare earths of the yttrium subgroup (*R* = Y, Gd, Dy, Ho, Er, Lu) [1,9-11,14,15] shows a reduction of the number of ternary compounds down to three for the Lu–Cu–Sn system, with the exception of the Yb–Cu–Sn system, where ten intermediate phases were found at 673 K [13]. In the case of Yb the structure and stoichiometry of some of the compounds are unique for the Yb–Cu–Sn system: $Yb_3Cu_6Sn_5$ ($Dy_3Co_6Sn_5$-type), $Yb_3Cu_8Sn_4$ ($Lu_3Co_{7.77}Sn_4$-type), $Yb_5Cu_{11}Sn_8$ (own structure type) [28], and $Yb_4Cu_2Sn_5$ (own structure type) [29].

Due to the low melting temperature of Sn (505 K) most *R*–Cu–Sn systems were studied at 670 K, particularly at high Sn content [1-15]. The use of a higher annealing temperature in the {Gd,Dy}–Cu–Sn systems [10,12] resulted in decomposition of the $R_2Cu_{4-x}Sn_{5+x}$ phases ($Sm_2Cu_4Sn_5$-type, space group *I*4*mm*), which exist at 670 K, while at 770 K they were not observed [30]. The influence of the temperature on the crystal structures of the $R_3Cu_4Sn_4$ compounds (*R* = Tm, Lu) leads to two structural modifications (monoclinic $Tm_3Cu_4Sn_4$-type and orthorhombic $Gd_3Cu_4Ge_4$-type) [14].

In the present paper the results of X-ray diffraction and EPM analyses of the phase equilibria in the Tb–Cu–Sn system at 670 K, crystallographic data of the ternary compounds, and the influence of different heat treatments on the stability of the ternary compounds, are reported.

2. Experimental

For our investigation the samples were synthesized by direct arc melting of the constituent metals (terbium, purity 99.9 wt.%; copper, purity 99.99 wt.%; and tin, purity 99.999 wt.%) under a high-purity Ti-gettered argon atmosphere on a water-cooled copper bottom. To ensure the homogeneity the alloys were re-melted twice. The weight losses of the total mass after melting were lower than 1 wt.%. Pieces of the as-cast buttons were annealed for one month at 670 K in evacuated silica ampoules. Samples with high Cu content (> 60 at.%) were annealed first at 870 K for two weeks, and at the next step at 670 K for another two weeks. Then the ampoules were quenched in ice water. All of the samples were stable in air.

For the characterization of the annealed samples, X-ray powder diffraction (XRPD, diffractometer DRON-4.0, Fe *Kα* radiation) was used. To check the phase composition of the alloys the observed diffraction intensities were compared with reference powder patterns of the pure elements, binary and known ternary phases. The chemical and phase compositions of the samples were examined by Scanning Electron Microscopy (SEM) using a REMMA-102-02 scanning microscope. Quantitative electron probe microanalysis (EPMA) of the samples with an accuracy of ~0.5-1.0 at.% was carried out by using an energy-dispersive X-ray analyzer with the pure elements as standards (standard acceleration voltage 20 kV; *K*- and *L*-lines were used). For structure calculation XRPD data were collected in the transmission mode on a STOE STADI P diffractometer (linear position-sensitive detector, $2\theta/\omega$-scan, Cu $K\alpha_1$ radiation, curved germanium (1 1 1) monochromator). Calculations of the crystallographic parameters were performed using the WinCSD and FullProf Suite program packages [31,32].

3. Results and discussion

3.1. Isothermal section of the Tb–Cu–Sn system

To study the phase relations in the Tb–Cu–Sn ternary system 15 binary and 29 ternary alloys were prepared, annealed at 670 K, and characterized by X-ray diffraction and scanning electron microscopy (SEM).

For our investigations data concerning the binary systems that delimit the studied Tb–Cu–Sn system were taken from the literature [33,34] (Tb–Cu and Cu–Sn), the data of the Tb–Sn binary system were found in [35,36]. In our work the presence of all the binary compounds reported in the Tb–Cu and Cu–Sn systems was confirmed at 670 K. In the ternary part of the system, the formation of a substitutional solid solution based on the binary compound $TbCu_5$ ($AuBe_5$-type) up to 5 at.% Sn was found (a = 0.7041(3) nm for $TbCu_5$, a = 0.7086(2) nm for the $Tb_{17}Cu_{78}Sn_5$ sample). The limiting composition of the $TbCu_{5-x}Sn_x$ solid solution was confirmed by EPMA data ($Tb_{17.51}Cu_{77.65}Sn_{4.84}$). The solubility of Sn in the binary phase TbCu (CsCl-type) extends up to ~2.6 at.% ($Tb_{50.90}Cu_{46.52}Sn_{2.58}$). In the Tb–Sn system samples with compositions corresponding to the literature data were synthesized and analyzed by X-ray powder diffraction. The analysis confirmed the existence of the Tb_5Sn_3 (Mn_5Si_3-type), Tb_5Sn_4 (Sm_5Ge_4-type), $Tb_{11}Sn_{10}$ ($Ho_{11}Ge_{10}$-type), $TbSn_2$ ($ZrSi_2$-type), Tb_3Sn_7 (Tb_3Sn_7-type), and $TbSn_3$ ($GdSn_{2.75}$-type) binaries. The results are in good agreement with the last version of the Tb–Sn phase diagram [36]. Two binary phases TbSn and Tb_4Sn_5 [37] were not identified at the temperature of annealing, the samples with the corresponding compositions contained the compounds $Tb_{11}Sn_{10}$ and $TbSn_2$ in equilibrium. Crystallographic characteristics of the Tb–Cu, Tb–Sn, and Cu–Sn binary compounds are given in Table 1.

The phase equilibrium diagram of the Tb–Cu–Sn system at 670 K was constructed based on the results of the X-ray diffraction and EPM analyses of the prepared alloys (Fig. 1). The phase compositions of selected samples are listed in Table 2, and SEM pictures of some alloys are shown in Figs. 2,3.

According to X-ray diffraction and EPMA data, the phase diagram of the Tb–Cu–Sn system at 670 K is characterized by the formation of five ternary compounds, the crystallographic characteristics of which are listed in Table 3. The refined lattice parameters of the confirmed compounds are in good agreement with literature data [24,25]. All the ternary compounds are characterized by narrow homogeneity ranges at the investigated temperature. No ternary compounds were observed in the ternary part Tb_5Sn_3–Tb–TbCu, where the alloys contain two (Tb_5Sn_3, TbCu) or three (Tb_5Sn_3, Tb, TbCu) phases in equilibrium (Fig. 1). The sample $Tb_{50}Cu_{40}Sn_{10}$ with low Tb content belongs to a three-phase field and contains Tb_5Sn_3, TbCu, and $TbCu_2$ (Fig. 2a). These results are consistent with Tb–Cu binary system [33], where compounds with a Tb content of more than 50 at.% do not form.

An interstitial-type solid solution $TbCu_xSn_2$ (up to 4 at.% Cu), based on the binary compound $TbSn_2$ ($ZrSi_2$-type), was observed as reported earlier [39] (a = 0.4397(4), b = 1.6211(2), c = 0.4326(3) nm for $Tb_{32}Cu_4Sn_{64}$). According to EPMA data the limiting composition of the $TbCu_xSn_2$ solid solution is $Tb_{32.72}Cu_{4.09}Sn_{63.19}$. The sample $Tb_{30}Cu_{10}Sn_{60}$ (Fig. 3a) with higher Cu content belongs to the three-phase field $Tb_3Cu_4Sn_4$–$TbCu_xSn_2$–Tb_3Sn_7. The limit of Cu

solubility in the $TbSn_2$ compound determined here is in an agreement with literature data [39]. Significant solubility of the third component in the other binary compounds was not observed under our conditions.

In a previous work [30] we established that the $Tb_2Cu_{3.5}Sn_{5.5}$ compound is stable up to ~400°C (670 K) (Fig. 4). At higher annealing temperatures this stannide decomposes. To check the influence of the temperature on the stability for the other compounds with low Sn content, we used a higher annealing temperature (Table 4). As a result, it was found that four ternary compounds are stable up to 1070 K (the higher annealing temperature used in our work).

The limit of the temperature stability of the $Tb_2Cu_{3.5}Sn_{5.5}$ compound (up to ~670 K) connects well with the phase diagram of the Cu–Sn system [33], which is characterized by low-temperature formation of binary phases in the region with more than 50 at.% Sn and by the presence of a large liquid region down to low temperatures.

Table 1 The binary phases relevant to the 670 K isothermal section of the Tb–Cu–Sn system.

Phase	Melting and transformation temperature (K) [a]	Pearson symbol, structure type	Lattice parameters, nm			Ref.
			a	*b*	*c*	
$TbSn_3$	p 721 K	*oS*16, $GdSn_{2.75}$	0.4347(3)	0.4388(5)	2.1917(6)	This work
Tb_3Sn_7	p 1019 K	*oS*28, Tb_3Sn_7	0.4363	2.6347	0.4441	[36]
$TbSn_2$	m 1431 K	*oS*12, $ZrSi_2$	0.4394(6)	1.6213(3)	0.4322(6)	This work
$Tb_{11}Sn_{10}$	p 1865 K	*tI*84, $Ho_{11}Ge_{10}$	1.1581(5)	–	1.6987(5)	This work
Tb_5Sn_4	p 1983 K	*oP*36, Sm_5Ge_4	0.8004	1.5418	0.8139	[35]
Tb_5Sn_3	m 2125 K	*hP*16, Mn_5Si_3	0.8948(3)	–	0.6534(3)	This work
Cu_3Sn	pm 949 K	*oP*8, Cu_3Ti	0.4317(3)	0.5488(5)	0.4736(4)	This work
$Cu_{41}Sn_{11}$	p 865 K	*cF*416, $Cu_{41}Sn_{11}$	1.7944	–	–	[38]
Cu_6Sn_5	pm 462 K	*mS*44, Cu_6Sn_5	1.1015(6)	0.7273(4) β = 98.8(1)°	0.9817(5)	This work
TbCu	m 1173 K	*cP*2, CsCl	0.3482(5)	–	–	This work
$TbCu_2$	m 1145 K	*oI*12, KHg_2	0.4315(3)	0.6888(4)	0.7324(5)	This work
$TbCu_5$	pm 1168 K	*cF*24, $AuBe_5$	0.7041(3)	–	–	This work

[a] p – peritectic reaction; m – congruent melting; pm – polymorphic transformation

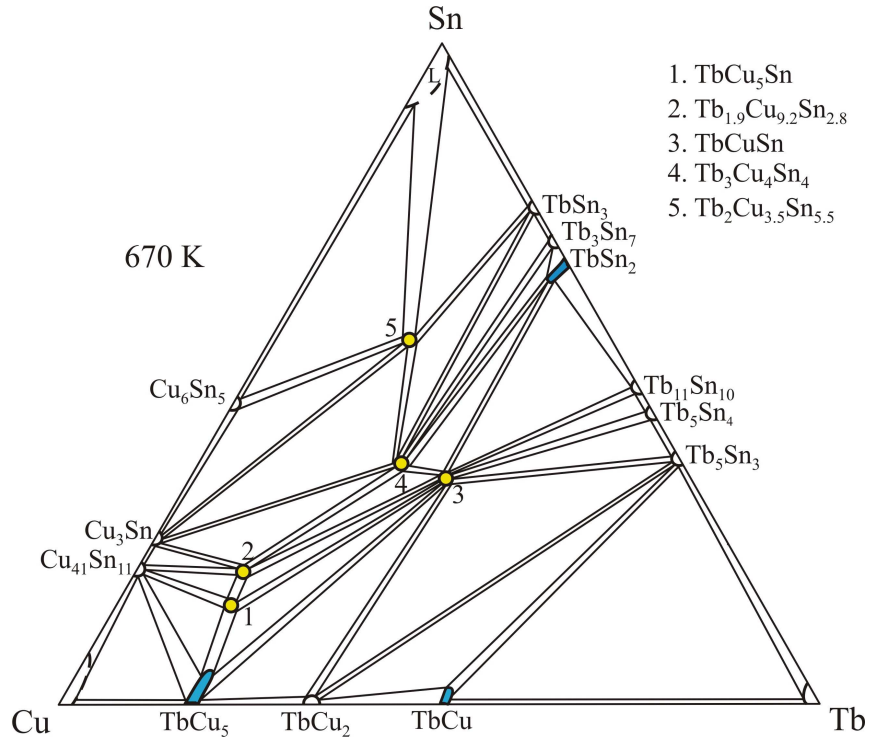

Fig. 1 Isothermal section of the Tb–Cu–Sn system at 670 K.

Table 2 Phase composition of selected Tb–Cu–Sn alloys (670 K).

No	Nominal composition of the alloy, at.%			Phases		
	Tb	Cu	Sn	1st phase	2nd phase	3rd phase
1	25	70	5	$TbCu_2$ a = 0.4318(4) nm b = 0.6888(3) nm c = 0.7322(5) nm	$TbCu_5$ a = 0.7049(3) nm	TbCuSn (traces)
2 (Fig. 2a)	50	40	10	$TbCu_{1-x}Sn_x$ $Tb_{50.90}Cu_{46.51}Sn_{2.59}$ a = 0.3482(2) nm	Tb_5Sn_3 $Tb_{63.11}Sn_{36.89}$ a = 0.8948(3) nm c = 0.6534(3) nm	$TbCu_2$ $Tb_{32.43}Cu_{67.57}$ a = 0.4315(3) nm b = 0.6888(4) nm c = 0.7324(5) nm
3 (Fig. 2b)	17	66	17	$TbCu_5Sn$ $Tb_{14.77}Cu_{70.87}Sn_{14.36}$ a = 0.8221(4) nm b = 0.4978(5) nm c = 1.0577(6) nm	$Tb_{1.9}Cu_{9.2}Sn_{2.8}$ $Tb_{14.09}Cu_{65.73}Sn_{20.18}$ a = 0.5036(4) nm c = 2.0413(6) nm	TbCuSn $Tb_{32.89}Cu_{33.41}Sn_{33.70}$ a = 0.4519(4) nm c = 0.7271(4) nm
4 (Fig. 2c)	35	45	20	TbCuSn $Tb_{33.12}Cu_{34.02}Sn_{32.86}$ a = 0.4518(3) nm c = 0.7270(4) nm	Tb_5Sn_3 $Tb_{62.93}Sn_{37.07}$ a = 0.8949(4) nm c = 0.6533(3) nm	$TbCu_2$ $Tb_{33.29}Cu_{66.71}$ a = 0.4317(4) nm b = 0.6889(4) nm c = 0.7323(5) nm
5	13	62	25	$Tb_3Cu_4Sn_4$ a = 0.4421(3) nm b = 0.6940(6) nm c = 1.4549(8) nm	$Tb_{1,9}Cu_{9.2}Sn_{2.8}$ a = 0.5035(3) nm c = 2.0415(5) nm	Cu_3Sn a = 0.4317(3) nm b = 0.5486(4) nm c = 0.4737(4) nm
6 (Fig. 2d)	13	57	30	$Tb_3Cu_4Sn_4$ $Tb_{27.12}Cu_{37.22}Sn_{35.66}$ a = 0.4423(2) nm b = 0.6940(4) nm c = 1.4551(6) nm	Cu_3Sn $Cu_{74.13}Sn_{25.87}$ a = 0.4317(3) nm b = 0.5486(4) nm c = 0.4737(4) nm	
7 (Fig. 3c)	17	58	25	$Tb_3Cu_4Sn_4$ $Tb_{26.77}Cu_{36.84}Sn_{36.39}$ a = 0.4422(3) nm b = 0.6941(5) nm c = 1.4549(7) nm	$Tb_{1.9}Cu_{9.2}Sn_{2.8}$ $Tb_{14.21}Cu_{66.10}Sn_{19.69}$ a = 0.5036(4) nm c = 2.0415(6) nm	
8 (Fig. 3b)	20	40	40	$Tb_3Cu_4Sn_4$ $Tb_{26.92}Cu_{36.67}Sn_{36.41}$ a = 0.4421(3) nm b = 0.6941(5) nm c = 1.4550(6) nm	$Tb_2Cu_{3.5}Sn_{5.5}$ $Tb_{17.78}Cu_{31.93}Sn_{50.29}$ a = 0.4405(4) nm c = 2.5854(5) nm	Cu_3Sn $Cu_{73.82}Sn_{26.18}$ a = 0.4317(3) nm b = 0.5486(4) nm c = 0.4737(4) nm
9	45	15	40	TbCuSn a = 0.4517(3) nm c = 0.7269(3) nm	$Tb_{11}Sn_{10}$ a = 1.1581(5) nm c = 1.6987(5) nm	Tb_5Sn_4 (traces)
10 (Fig. 3d)	25	25	50	$Tb_3Cu_4Sn_4$ $Tb_{27.02}Cu_{36.87}Sn_{37.11}$ a = 0.4420(3) nm b = 0.6940(4) nm c = 1.4551(5) nm	$Tb_2Cu_{3.5}Sn_{5.5}$ $Tb_{18.23}Cu_{31.88}Sn_{49.89}$ a = 0.4404(4) nm c = 2.5855(6) nm	$TbSn_3$ $Tb_{24.17}Sn_{75.83}$ a = 0.4347(3) nm b = 0.4388(5) nm c = 2.1917(6) nm
11	13	37	50	$Tb_2Cu_{3.5}Sn_{5.5}$ a = 0.4404(4) nm c = 2.5855(6) nm	Cu_3Sn a = 0.4317(3) nm b = 0.5486(4) nm c = 0.4737(4) nm	Cu_6Sn_5 a = 1.1022 nm b = 0.7282 nm c = 0.9827 nm β = 98.84

Table 2 Phase composition of selected Tb–Cu–Sn alloys (670 K) (continued).

No	Nominal composition of the alloys, at.%			Phases		
	Tb	Cu	Sn	1st phase	2nd phase	3rd phase
12	10	35	55	$Tb_2Cu_{3.5}Sn_{5.5}$ *a* = 0.4404(4) nm *c* = 2.5855(6) nm	Cu_6Sn_5 *a* = 1.1022 nm *b* = 0.7282 nm *c* = 0.9827 nm β = 98.84	(Sn) *a* = 0.5808(4) nm *c* = 0.3177(5) nm
13 (Fig. 3a)	30	10	60	$Tb_3Cu_4Sn_4$ $Tb_{27.15}Cu_{36.64}Sn_{36.21}$ *a* = 0.4420(3) nm *b* = 0.6941(3) nm *c* = 1.4551(5) nm	$TbCu_xSn_2$ $Tb_{32.14}Cu_{4.10}Sn_{63.76}$ *a* = 0.4394(6) nm *b* = 1.6213(3) nm *c* = 0.4322(6) nm	Tb_3Sn_7 $Tb_{29.69}Sn_{70.31}$ (traces)

Table 3 Crystallographic characteristics of the ternary compounds in the Tb–Cu–Sn system.

Compound	Space group	Structure type	Lattice parameters, nm		
			a	*b*	*c*
$TbCu_5Sn$	*Pnma*	$CeCu_5Au$	0.82205(1)	0.49789(3)	1.05766(6)
$Tb_{1.9}Cu_{9.2}Sn_{2.8}$	*P*6$_3$/*mmc*	$Dy_{1.9}Cu_{9.2}Sn_{2.8}$	0.50355(9)	–	2.0414(6)
TbCuSn	*P*6$_3$*mc*	LiGaGe	0.4517(2)	–	0.7272(3)
$Tb_3Cu_4Sn_4$	*Immm*	$Gd_3Cu_4Ge_4$	0.4421(3)	0.6939(3)	1.4547(5)
$Tb_2Cu_{3.5}Sn_{5.5}$	*I*4*mm*	$Sm_2Cu_4Sn_5$	0.4404(4)	–	2.5854(3)

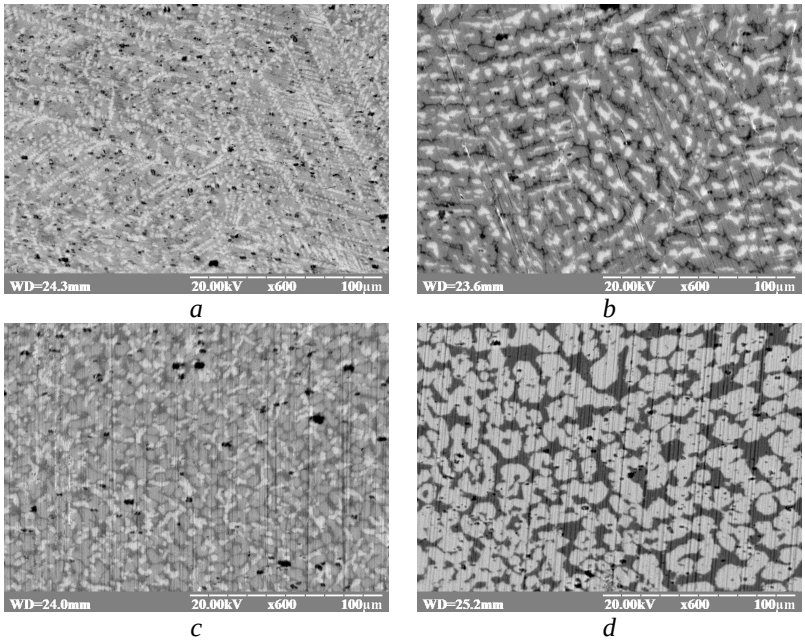

a *b* *c* *d*

Fig. 2 SEM pictures of alloys from the Tb–Cu–Sn system: *a*) $Tb_{50}Cu_{40}Sn_{10}$ ($TbCu_{1-x}Sn_x$ – gray phase, $TbCu_2$ – dark phase, Tb_5Sn_3 – light phase); *b*) $Tb_{17}Cu_{66}Sn_{17}$ ($TbCu_5Sn$ – gray phase, TbCuSn – light phase, $Tb_{1.9}Cu_{9.2}Sn_{2.8}$ – dark phase); *c*) $Tb_{35}Cu_{45}Sn_{20}$ (TbCuSn – gray phase, Tb_5Sn_3 – light phase, $TbCu_2$ – dark phase); *d*) $Tb_{13}Cu_{57}Sn_{30}$ ($Tb_3Cu_4Sn_4$ – light phase, Cu_3Sn – dark phase).

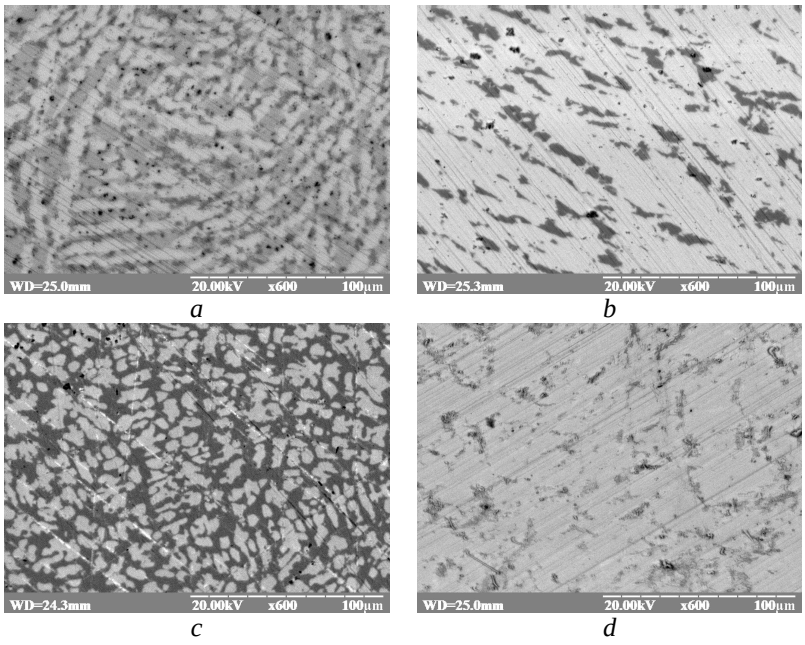

Fig. 3 SEM pictures of alloys from the Tb–Cu–Sn system: *a*) $Tb_{30}Cu_{10}Sn_{60}$ ($Tb_3Cu_4Sn_4$ – gray phase, $TbCu_xSn_2$ – light phase, Tb_3Sn_7 – dark gray dark phase); *b*) $Tb_{20}Cu_{40}Sn_{40}$ ($Tb_3Cu_4Sn_4$ – gray phase, $Tb_2Cu_{3.5}Sn_{5.5}$ – light phase, Cu_3Sn – dark phase); *c*) $Tb_{17}Cu_{58}Sn_{25}$ ($Tb_3Cu_4Sn_4$ – light phase, $Tb_{1.9}Cu_{9.2}Sn_{2.8}$ – dark phase); *d)* $Tb_{25}Cu_{25}Sn_{50}$ ($Tb_3Cu_4Sn_4$ – gray phase; $Tb_2Cu_{3.5}Sn_{5.5}$ – light phase, $TbSn_3$ – dark phase).

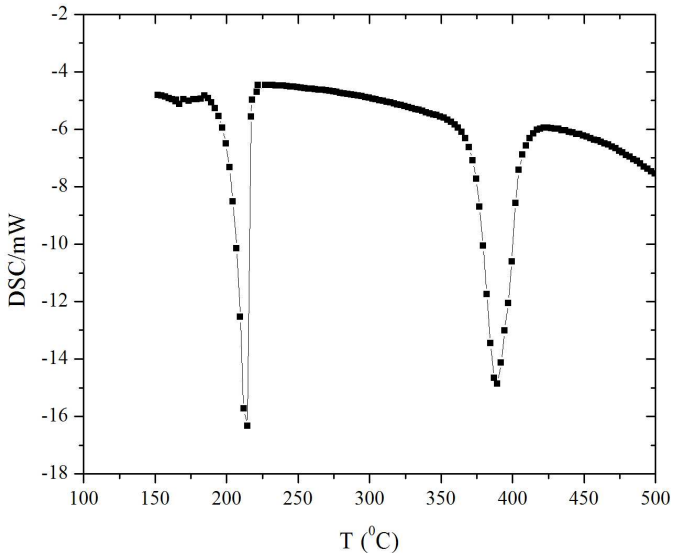

Fig. 4 DSC curve for the $Tb_2Cu_{3.5}Sn_{5.5}$ compound [30].

Table 4 Phases observed after different heat treatments in the Tb–Cu–Sn system.

Annealing temperature / time			
670 K / four weeks	770 K / four weeks	870 K / four weeks	1070 K / two weeks
$TbCu_5Sn$	$TbCu_5Sn$	$TbCu_5Sn$	$TbCu_5Sn$
$Tb_{1.9}Cu_{9.2}Sn_{2.8}$	$Tb_{1.9}Cu_{9.2}Sn_{2.8}$	$Tb_{1.9}Cu_{9.2}Sn_{2.8}$	$Tb_{1.9}Cu_{9.2}Sn_{2.8}$
TbCuSn	TbCuSn	TbCuSn	TbCuSn
$Tb_3Cu_4Sn_4$	$Tb_3Cu_4Sn_4$	$Tb_3Cu_4Sn_4$	$Tb_3Cu_4Sn_4$
$Tb_2Cu_{3.5}Sn_{5.5}$	–	–	–

3.2. Structural study

In the Cu-rich corner of the *R*–Cu–Sn systems the formation of the RCu_5Sn and $R_{1.9}Cu_{9.2}Sn_{2.8}$ (*R* = Y, Ce-Nd, Sm, Gd-Lu) compounds was found [40,41]. The presence of the corresponding compounds $TbCu_5Sn$ and $Tb_{1.9}Cu_{9.2}Sn_{2.8}$ was confirmed in our study (see Fig. 1).

We recently performed detailed structural studies of the $TbCu_5Sn$ stannide (X-ray powder diffraction method) and established that this compound belongs to the $CeCu_5Au$ type (ordered variant of the $CeCu_6$-type, space group *Pnma*) with ordered distribution of all the atoms in the structure [42]. The stoichiometry 1:5:1 of the compound was confirmed by EPMA data (see Table 2, Fig. 2b, $Tb_{14.77}Cu_{70.87}Sn_{14.36}$).

During the present work, the crystal structure of the $Tb_{1.9}Cu_{9.2}Sn_{2.8}$ stannide was refined by X-ray powder diffraction. Detailed crystal structure refinements were performed for the $Tb_{13}Cu_{67}Sn_{20}$ sample, using as starting model the $Dy_{1.9}Cu_{9.2}Sn_{2.8}$ structure type (space group $P6_3/mmc$, disordered variant of the $CeNi_5Sn$ structure type). Experimental details of the structure refinements are summarized in Table 5. Refined atomic coordinates and displacement parameters are listed in Table 6. The refinements of the site occupancies showed that the occupancy of site Tb1 in Wyckoff position 2*d* is 0.88, and the site in 2*c* is occupied by a statistical mixture Sn/Cu. Thus, the chemical formula of the compound should be written as $Tb_{1.9}Cu_{9.2}Sn_{2.8}$ and is in a good agreement with electron probe microanalysis ($Tb_{13.60}Cu_{66.32}Sn_{20.08}$).

No homogeneity range was found for this stannide. The observed, calculated and difference X-ray patterns of the $Tb_{1.9}Cu_{9.2}Sn_{2.8}$ compound are shown in Fig. 5. The interatomic distances in the structure are close to the sum of the atomic radii of the components. Some shortening was observed for the interatomic distances Cu1-Cu1 (0.2457 nm), Cu2-Sn3 (0.2651 nm), and Tb-(Sn/Cu) (0.2909 nm).

Table 5 Experimental details and crystallographic data for the $Tb_{1.9}Cu_{9.2}Sn_{2.8}$ stannide.

Alloy composition	$Tb_{13}Cu_{67}Sn_{20}$
Refined composition	$Tb_{1.9}Cu_{9.2}Sn_{2.8}$
EPMA composition	$Tb_{13.60}Cu_{66.32}Sn_{20.08}$
Space group	$P6_3/mmc$ (No. 194)
Pearson symbol	*hP*28
Z	4
Cell parameters: *a*, nm	0.50355(9)
c, nm	2.0414(6)
Calculated density D_x, g/cm^3	9.067
Diffractometer	STOE STADI P (transmission mode, curved Ge(111) monochromator on primary beam)
Radiation, wavelength λ, Å	Cu $K\alpha_1$, 1.540598
Angular range for data collection / increment, °	$6.000 \le 2\theta \le 110.625$ / 0.015
Half-width parameters: *U*	0.004(1)
V	-0.010(7)
W	0.015(5)
Asymmetry parameters: P_1	0.069(4)
P_2	0.018(7)
Reliability factors: R_{Bragg}	0.0566
R_F	0.0561

Table 6 Atomic positional and isotropic displacement parameters for the $Tb_{1.9}Cu_{9.2}Sn_{2.8}$ compound.

Atom	Wyckoff position	*x*/*a*	*y*/*b*	*z*/*c*	$B_{iso}\cdot 10^2$, nm^2	Occupancy
Tb1	2*d*	⅓	⅔	¾	1.17(8)	0.88
Tb2	2*a*	0	0	0	1.22(6)	1
Cu1	12*k*	0.1650(4)	0.3300(1)	0.1427(1)	0.33(1)	1
Cu2	4*f*	⅓	⅔	0.0400(2)	1.25(1)	1
Cu3	2*b*	0	0	¼	1.11(1)	1
Sn	4*f*	⅓	⅔	0.5854(1)	0.64(5)	1
(Sn/Cu)	2*c*	⅓	⅔	¼	1.42(9)	0.82/0.18

The structures of both the $TbCu_5Sn$ and $Tb_{1.9}Cu_{9.2}Sn_{2.8}$ phases are derivatives of the hexagonal $CaCu_5$ structure type. With regard to the Tb–Cu phase diagram [33] the $TbCu_5$ binary with two polymorphic forms (low-temperature $AuBe_5$-type, high-temperature $CaCu_5$-type) forms in the Cu-rich corner. Under the conditions used in our work the $TbCu_5$ phase crystallizes in the cubic $AuBe_5$ structure type. In the ternary Cu-rich part of the Tb–Cu–Sn system incorporation of tin promotes the formation of the ternary stannides $TbCu_5Sn$ and $Tb_{1.9}Cu_{9.2}Sn_{2.8}$ with structures being derivatives of the $CaCu_5$ structure type (the high-temperature modification of the $TbCu_5$ phase belongs to the $CaCu_5$-type). The main building block in the structures of $TbCu_5Sn$ and $Tb_{1.9}Cu_{9.2}Sn_{2.8}$ is a hexagonal prism with six additional atoms, formed by Sn and in some cases Cu atoms, around the Tb atom (Fig. 6).

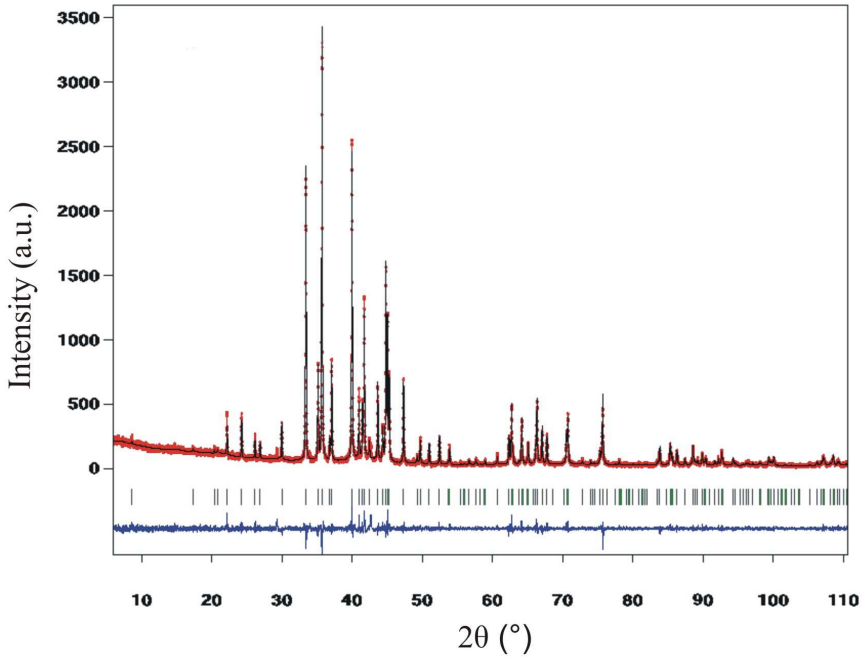

Fig. 5 The observed, calculated, and difference in X-ray patterns of the $Tb_{1.9}Cu_{9.2}Sn_{2.8}$ compound.

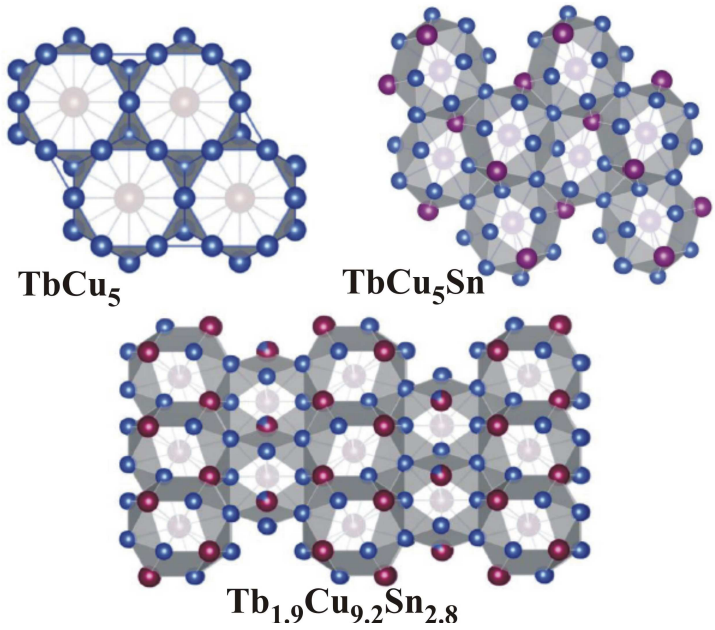

Fig. 6 Stacking of polyhedra in the $TbCu_5Sn$ and $Tb_{1.9}Cu_{9.2}Sn_{2.8}$ compounds.

Conclusions

The interaction between the components in the Tb–Cu–Sn system investigated here and previously studied *R*–Cu–Sn systems with heavy rare earths showed a close analogy in the stoichiometry and crystal structure of most of the formed ternary compounds (except for the Yb–Cu–Sn system). The similarity in the interaction of the elements in these systems is demonstrated by the formation of the compounds *R*CuSn, $R_3Cu_4Sn_4$, $R_{1.9}Cu_{9.2}Sn_{2.8}$, and RCu_5Sn (exception: the Lu–Cu–Sn system). Stannides with the $Sm_2Cu_4Sn_5$ structure type are formed in the systems with Gd, Tb, and Dy and are characterized by a limited temperature range of stability. Stannides with $MgCu_4Sn$-type structures were only observed in the Y–Cu–Sn and Yb–Cu–Sn systems.

Like the $HoCu_5Sn$ stannide [42] the crystal structure of the $TbCu_5Sn$ compound is characterized by ordered distribution of all the atoms corresponding to the $CeCu_5Au$-type, differing thus from the previously reported isotypic compound with Er ($CeCu_6$-type) the composition of which weakly deviates from $ErCu_5Sn$ ($ErCu_{4.5}Sn_{1.5}$) [40]. No homogeneity range was observed for the ternary compounds in the Tb–Cu–Sn system at 670 K.

Acknowledgments

We would like to acknowledge financial support of the Ministry of Education and Science of Ukraine under Grant No. 0121U109766.

References

[1] L. Romaka, I. Romaniv, Yu. Stadnyk, V.V. Romaka, R. Serkiz, R. Gladyshevskii, *Chem. Met. Alloys* 7 (2014) 132-138. https://doi.org/10.30970/cma7.0283

[2] Y. Zhan, H. Xie, J. Jiang, Y. Xu, Y. Wang, Y. Zhuang, *J. Alloys Compd.* 461 **(**2008) 570-573. https://doi.org/10.1016/j.jallcom.2007.07.040

[3] P. Riani, D. Mazzone, G. Zanicchi, R. Marazza, R. Ferro, F. Faudot, M. Harmelin, *J. Phase Equilib.* 3 (1998) 239-251. https://doi.org/10.1361/105497198770342256

[4] L.P. Komarovskaya, L.A. Mykhajliv, R.V. Skolozdra, *Izv. Akad. Nauk SSSR, Met.* 4 (1989) 209-213.

[5] P. Riani, D. Mazzone, G. Zanicchi, R. Marazza, R. Ferro, *Intermetallics* 8 (2000) 259-266. https://doi.org/10.1016/S0966-9795(99)00101-6

[6] D. Mazzone, P.L. Paulose, S.K. Dhar, M.L. Fornasini, P. Manfrinetti, *J. Alloys Compd.* 453 (2008) 24-31. https://doi.org/10.1016/j.jallcom.2006.11.094

[7] P. Riani, D. Mazzone, G. Zanicchi, R. Marazza, *J. Alloys Compd.* 247 (1997) 148-153. https://doi.org/10.1016/S0925-8388(96)02607-2

[8] P. Riani, M.L. Fornasini, R. Marazza, D. Mazzone, G. Zanicchi, R. Ferro, *Intermetallics* 7 (1999) 835-846. https://doi.org/10.1016/S0966-9795(98)00132-0

[9] I.V. Senkovska, Ya.S. Mudryk, L.P. Romaka, O.I. Bodak, *J. Alloys Compd.* 312 (2000) 124-129. https://doi.org/10.1016/S0925-8388(00)01092-6

[10] L. Romaka, V.V. Romaka, E.K. Hlil, D. Fruchart, *Chem. Met. Alloys* 2 (2009) 68-74. https://doi.org/10.30970/cma2.0095

[11] O.I. Bodak, V.V. Romaka, L.P. Romaka, A.V. Tkachuk, Yu.V. Stadnyk, *J. Alloys Compd.* 395 (2005) 113-116. https://doi.org/10.1016/j.jallcom.2004.11.042

[12] V. Romaka, Yu. Gorelenko, L. Romaka, *Visn. Lviv. Univ., Ser. Khim.* 49 (2008) 3-9.

[13] G. Zanicchi, D. Mazzone, M.L. Fornasini, P. Riani, R. Marazza, R. Ferro, *Intermetallics* 7 (1999) 957-966. https://doi.org/10.1016/S0966-9795(99)00003-5

[14] L. Romaka, V.V. Romaka, V. Davydov, *Chem. Met. Alloys* 1(2) (2008) 192-197. https://doi.org/10.30970/cma1.0058

[15] L. Romaka, I. Romaniv, V.V. Romaka, M. Konyk, A. Horyn, Yu. Stadnyk, *Phys. Chem. Solid State* 19(2) (2018) 139-146. https://doi.org/10.15330/pcss.19.2.139-146

[16] C.P. Sebastian, C. Fehse, H. Eckert, R.D. Hoffmann, R. Pöttgen, *Solid State Sci.* 8(11) (2006) 1386-1392. https://doi.org/10.1016/j.solidstatesciences.2006.07.006

[17] J.P. Maehlen, M. Stange, V.A. Yartys', R.G. Delaplane, *J. Alloys Compd.* 404 (2005) 112-117. https://doi.org/10.1016/j.jallcom.2004.09.086

[18] J.V. Pacheco, K. Yvon, E. Gratz, *Z. Kristallogr.* 213 (1998) 510-512. https://doi.org/10.1524/zkri.1998.213.10.510

[19] S. Baran, V. Ivanov, J. Leciejewicz, N. Stusser, A. Szytula, A. Zygmunt, Y.F. Ding, *J. Alloys Compd.* 257 (1997) 5-13. https://doi.org/10.1016/S0925-8388(96)02731-4

[20] R. Pöttgen, *J. Alloys Compd.* 243 (1996) L1-L4. https://doi.org/10.1016/S0925-8388(96)02354-7

[21] K. Katon, T. Takabatake, A. Minami, I. Oguro, H. Sawa, *J. Alloys Compd.* 261 (1997) 32-36. https://doi.org/10.1016/S0925-8388(97)00194-1

[22] F. Yang, J.P. Kuang, J. Li, E. Bruck, H. Nakotte, F.R. de Boer, X. Wu, Z. Li, Y. Wang, *J. Appl. Phys.* 69(8) (1991) 4705-4707. https://doi.org/10.1063/1.348279

[23] C.P. Sebastian, S. Rayaprol, R.-D. Hoffmann, U.C. Rodewald, T. Pape, R. Pöttgen, *Z. Naturforsch. B* 62 (2007) 647-657. https://doi.org/10.1515/znb-2007-0504

[24] R.V Skolozdra: in: K.A. Gschneidner, Jr. and L. Eyring (Eds.), Handbook on the Physics and Chemistry of Rare Earths, Vol. 24, 1997.
[25] V.V. Romaka, L.P. Romaka, V.Ya. Krajovskyj, Yu.V. Stadnyk, *Stannides of rare earth and transition metals.* Lviv Polytech. Univ. 2015, 221 p.
[26] L.P. Komarovskaya, S.A. Sadykov, R.V. Skolozdra, *Izv. Akad. Nauk SSSR, Met.* 33(8) (1988) 1249-1251.
[27] S. Singh, M.L. Fornasini, P. Manfrinetti, A. Palenzona, S.K. Dhar, P.L. Paulose, *J. Alloys Compd.* 317-318 **(**2001) 560-566. https://doi.org/10.1016/S0925-8388(00)01388-8
[28] M.L. Fornasini, P. Manfrinetti, D. Mazzone, P. Riani, G. Zanicchi, *J. Solid State Chem.* 177 (2004) 1919-1924. https://doi.org/10.1016/j.jssc.2004.02.007
[29] M.L. Fornasini, G. Zanicchi, D. Mazzone, P. Riani, *Z. Kristallogr*. 216(1) (2001) 21-22. https://doi.org/10.1524/ncrs.2001.216.14.21
[30] V.V. Romaka, D. Gignoux, L. Romaka, N. Skryabina, D. Fruchart, Yu. Stadnyk, *J. Alloys Compd.* 509 **(**2011) 5206-5210. https://doi.org/10.1016/j.jallcom.2011.02.055
[31] L. Akselrud, Yu. Grin, WinCSD: software package for crystallographic calculations (Version 4). *J. Appl. Crystallogr*. 47 (2014) 803-805. https://doi.org/10.1107/S1600576714001058
[32] J. Rodriguez-Carvajal, *Commission on Powder Diffraction (IUCr), Newsletters* 26 (2001) 12.
[33] T. Massalski (Ed.), *Binary Alloy Phase Diagrams*. ASM, Metals Park, Ohio 1990.
[34] Villars P., Calvert L. (Eds.), *Pearson's Handbook of Crystallographic Data for Intermetallic Phases*, ASM, Materials Park, Ohio, USA, 1991.
[35] V.N. Eremenko, M.V. Bulanova, P.S. Martsenyuk, *Dopov. Akad. Nauk Ukr. RSR, Ser. B* 1 (1990) 35-37.
[36] A. Palenzona, P. Manfrinetti, *J. Alloys Compd*. 201 (1993) 43-47. https://doi.org/10.1016/0925-8388(93)90859-L
[37] V.N. Eremenko, M.V. Bulanova, P.S. Martsenyuk, *Ukr. Khim. Zh.* 57(3) (1990) 14-18.
[38] S. Fürtauer, D. Li, D. Cupid, H. Flandorfer, *Intermetallics* 34 (2013) 142-147. https://doi.org/10.1016/j.intermet.2012.10.004
[39] M. François, G. Venturini, B. Malaman, B. Roques, *J. Less-Common Met*. 160 (1990) 197-213. https://doi.org/10.1016/0022-5088(90)90381-S
[40] Ya. Mudryk, O. Isnard, L. Romaka, D. Fruchart, *Solid State Commun.* 119 (2001) 423-427. https://doi.org/10.1016/S0038-1098(01)00273-3
[41] V.V. Romaka, D. Fruchart, R. Gladyshevskii, P. Rogl, N. Koblyuk, *J. Alloys Compd.* 460 (2008) 283-288. https://doi.org/10.1016/j.jallcom.2007.06.022
[42] I. Romaniv, L. Romaka, B. Kuzhel, V.V. Romaka, M. Rudchenko, Yu. Stadnyk, M. Konyk, M. Rudko, *Chem. Met. Alloys* 12(1/2) (2019) 1-8. https://doi.org/10.30970/cma12.0374